

**Molecular Conducting Magnetic Heterostructure**

Journal:	<i>Journal of Materials Chemistry C</i>
Manuscript ID	TC-COM-10-2019-005450.R2
Article Type:	Communication
Date Submitted by the Author:	13-Dec-2019
Complete List of Authors:	Hu, Feng; University at Buffalo - The State University of New York Hu, Yong ; University at Buffalo - The State University of New York Huang, Yulong; University at Buffalo - The State University of New York, Mechanical & Aerospace Engineering Li, Changning; University at Buffalo - The State University of New York, School of Engineering and Applied Sciences Yang, Ruizhe; University at Buffalo - The State University of New York Ren, Shenqiang; University at Buffalo - The State University of New York,

## COMMUNICATION

## Molecular Conducting Magnetic Heterostructure

Feng Hu, Yong Hu, Yulong Huang, Changning Li, Ruizhe Yang, Shenqiang Ren\*

Received 00th January 20xx,

Accepted 00th January 20xx

DOI: 10.1039/x0xx00000x

**Building molecular conducting magnets has been considerable interest due to its metallic transport and magnetic properties. Conjugated aniline anions and transition metal cations are recognized to synthesize such  $\pi$ -d interaction frameworks. Here, an interfacial assembly of quasi-two-dimensional aniline heterojunction frameworks is developed, which consists of proton-aniline conducting layer (conductivity of  $9.2 \times 10^2 \text{ S cm}^{-1}$ ) and transition metal-aniline magnetic layer. The two-dimensional aniline coordination framework with the pronounced  $\pi$ -d interaction is indispensable to obtain the ordered spin states and metallic transport conductivity. We apply optical and Raman spectra to study the interaction between metal cation and the nitrogen atoms in the aniline chains. The bilayer heterostructure maintains a high conductivity of  $3.5 \times 10^2 \text{ S cm}^{-1}$  and an increased magnetization, while the coupling of metallic conducting and magnetic layers leads to an enhanced magnetoconductance of 0.4% under magnetic field of 70 kOe.**

Multifunctional materials with the charge and spin degree of freedom, such as molecular conducting magnets, are receiving significant interests as potentially transformative components in quantum technologies.<sup>[1]</sup> In this context, molecular conducting magnet is particularly attractive due to the coupling of molecular conductor and magnet, in which the magnetic interactions are triggered between the  $\pi$  conduction electrons and localized d electrons. Molecular conducting magnets prepared so far are mainly radical salts between low-dimensional conjugated donor molecules and magnetic acceptor anions.<sup>[2]</sup> Such molecular magnets are generally characterized as strongly correlated materials with  $\pi$  electron dominant transport due to its small transfer integral from the neighboring  $\pi$ -electron orbitals in donor molecules.<sup>[3]</sup> Such

unique packing structures enables the formation of a direct d-d spin interaction of magnetic anions and indirect  $\pi$ -d interaction between  $\pi$  conjugated cation and d electrons for electron transport. Magnetic ordering in the anion layer can be obtained by the combined effect of d-d and  $\pi$ -d interactions.<sup>[4]</sup> However, the  $\pi$ -d interaction could reduce electron mobility in the conjugated layer. In addition, the antiferromagnetic ordering is usually expected from the d-d interaction in such  $\pi$ -d system, while ferromagnetic ordering of d electrons can be resulted from the spin polarized  $\pi$  electrons.

Supramolecular assembly emerges as an effective approach to design and synthesize molecular conducting magnets from molecular synthons of alternately stacked  $\pi$ -conjugated donor molecules and transition-metal d-spin anion layers. Here we present a facile strategy to prepare freestanding molecular conducting magnets by self-assembly of quasi-two-dimensional aniline conjugated cation layer and transition metal anion layer. Polyaniline (PANI), selected here as one of the extensively investigated polymer materials, exhibits metallic transport, induced magnetic property, and remarkable environmental stability.<sup>[5]</sup> PANi is considered as Bronsted base and Lewis base, which can be doped to significantly improve metallic transport or magnetic property through coordination with Bronsted acid (HCl) or Lewis acid (transition metal halides) for the formation of conducting and magnetic building unit layers, respectively. The self-assembly driven chain ordering of quasi-two-dimensional nanosheets greatly increase the effects of magnetic alignment. The proton doped PANi has a significantly increased conductivity, while the iron cation incorporated PANi shows ferromagnetism-like behavior. More importantly, the conducting magnetic bilayer heterostructure can maintain a high conductivity and an enhanced magnetization due to the induced localized spin ordered states at the interface. When a magnetic field is applied to molecular conductor, the aligned d electrons induce ferromagnetic ordering together with the disrupted  $\pi$ -d interaction for the enhanced electron mobility, leading to the magneto-conductance effect.

Department of Mechanical and Aerospace Engineering, Chemistry, Research and Education in Energy, Environment & Water (RENEW), University at Buffalo, State University of New York, Buffalo, New York 14260, United States  
E-mail: [shenren@buffalo.edu](mailto:shenren@buffalo.edu)

Electronic Supplementary Information (ESI) available: [details of any supplementary information available should be included here]. See DOI: 10.1039/x0xx00000x

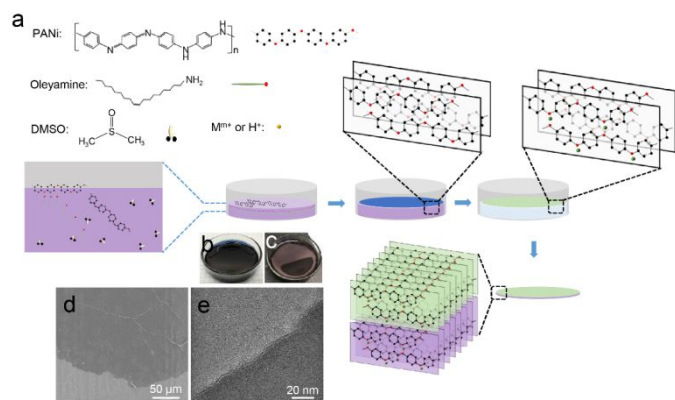


**Figure 1.** a) Illustration of the synthetic procedure for 2D PANi nanosheet on DMSO solution and doping process as well as the assembly of multifunctional conducting magnetic heterostructures. b, c) Photographs of DMSO solution before and after the PANi formation. d) SEM and e) TEM images of the PANi nanosheet.

The oleylamine molecule is a known surfactant for the controlled assembly due to the strong binding effect between the amino function with the surface atoms and the hydrophobic interaction of hydrocarbon chain.<sup>[6]</sup> Here, we report for the first time to utilize self-assembled oleylamine monolayer as the substrate to induce the ordering of aniline chain at the liquid/air interface. Figure 1a depicts the assembly process of freestanding quasi-two-dimensional PANi nanosheets at the dimethyl sulfoxide (DMSO)/air interface. Increased amount of oleylamine accelerates the assembly process of PANi formation (Figure S1 and S2). The as-formed freestanding PANi nanosheets can be transferred to transition metal salt or acid solution for the formation of magnetic or conductive PANi networks binding with imine and amine nitrogens, with the completion color changing from purple to green. Such coordinated PANi networks can be further layer-by-layer assembled for the formation of molecular conducting magnetic heterostructures. The optical photographs in Figure 1b and c show the PANi solution and self-assembled PANi nanosheet at the air-liquid interface. The scanning electron microscopy (SEM) image (Figure 1d) shows the uniform and flexible surface morphology of PANi nanosheets, while transmission electron microscopy (TEM, Figure 1e and S3) suggests its layer-like morphology.

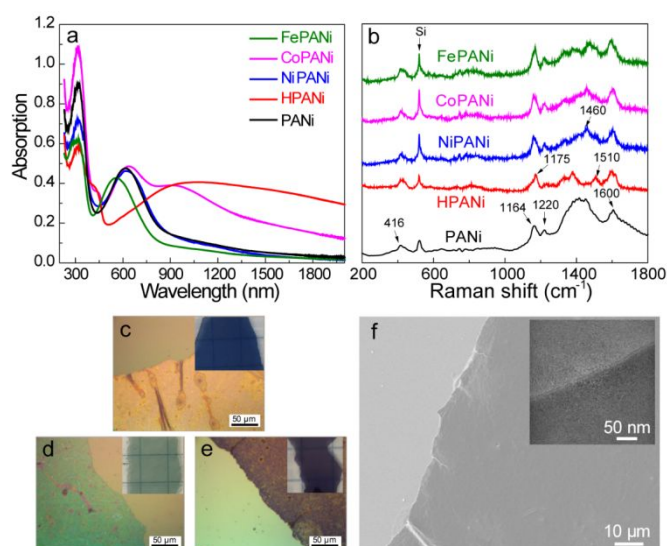


**Figure 2.** a) Absorption spectra of PANi, HCl-doped PANi (HPANi), and transition metal-doped PANi (MPANi). b) Raman spectra of PANi, HPANi, and MPANi. c-e) Photographs and corresponding optical microscopy images (Insets) of PANi, HPANi, and FePANi on glass substrates. f) SEM and TEM image (Inset) of FePANi.

The freestanding PANi nanosheets provide a versatile platform for the incorporation of transition metal cations and proton to control its physicochemical properties. Figure 2a shows the absorption spectra of freestanding PANi, HCl-doped PANi (HPANi), and transition metal-doped PANi (MPANi) nanosheets. The absorption band at 312 nm of self-assembled PANi nanosheet is assigned to the  $\pi-\pi^*$  transition of the conjugated benzenoid rings.<sup>[7]</sup> The  $\pi-\pi^*$  transition band shows a hypsochromic shift from 312 nm to 299 nm after Fe cation doping, suggesting a decrease in the extent of conjugation and an increase in the band gap. It is inferred that the adjacent phenyl rings of the aniline have larger torsion angles with respect to the plane of the nitrogen atoms due to the possible steric repulsion between the  $FeCl_3$  and hydrogens on the adjacent phenyl rings.<sup>[8]</sup> For the proton doping and other transition metal ions ( $NiCl_2$  and  $CoCl_2$ ), the  $\pi-\pi^*$  transition band shows negligible shift indicating the low steric repulsion possibly due to the weak binding interaction. The absorption band at 620 nm of self-assembled PANi nanosheet corresponds to the exciton transition.<sup>[9]</sup> The exciton transition band in transition metal doped PANi shows a blue shift to 560 nm after the Fe cation doping. It is inferred that  $Fe^{3+}$  ions strongly interact with the PANi chain increasing the degree of freedom and therefore the loss of planarity of the chain.<sup>[8]</sup> For the  $Co^{2+}$  doping, there are two new absorption bands located at 430 nm and 900 nm corresponding to the polaron and bipolaron transition in the doped form,<sup>[9]</sup> respectively, which are not observed in the  $Ni^{2+}$  doping. For the proton doping, the exciton transition band disappears while the bipolaron transition band exhibits a bathochromic shift comparing to the  $Co^{2+}$ -doped PANi indicating a conductive structure with a more delocalized bipolaron transition band.<sup>[9-10]</sup> Raman spectroscopy is further used to investigate self-assembled structural conformation and

interaction between dopants and aniline matrix chains. As shown in Figure 2b, the resonance Raman spectra of PANi, HPANi, and MPANi nanosheets are recorded using 785 nm excitation. The resonance bands that appeared in the range from  $\sim 1,160\text{ cm}^{-1}$  to  $1,600\text{ cm}^{-1}$  correspond to the stretching modes of different bonds in PANi.<sup>[11]</sup> Raman peak of  $1,600\text{ cm}^{-1}$  in PANi is assigned to the C-C stretching vibration of benzene rings. The bands at  $1,220\text{ cm}^{-1}$  and  $1,164\text{ cm}^{-1}$  are assigned to C-N stretching in benzenoid units and C-H deformation vibration of a quinonoid ring.<sup>[12]</sup> To evidence the effect of doping on the structure of PANi, on the one hand, the band at  $1,510\text{ cm}^{-1}$  in HPANi corresponds to N-H deformation vibrations, which is not observed in MPANi due to the doping of transition metal ions. On the other hand, the band at  $1,460\text{ cm}^{-1}$  corresponds to the C=N stretching vibrations in quinonoid units in MPANi, which is absent in HPANi indicating the more benzenoid units in the complex coordinated networks. As shown in Figure 2c-e, the as-formed PANi has blue color which can be converted to green color and purple color by proton doping and Fe cation doping, respectively. The SEM image in Figure 2f of Fe cation-doped PANi shows the similar morphology as the PANi. The EDS mapping (C and Fe elements) of Fe cation-doped PANi indicating the uniform doping of  $\text{Fe}^{3+}$  throughout the PANi network, while the HPANi nanosheet only shows the C and N elements (Figure S4 and S5). No visible iron cluster or particles are observed in TEM image (Inset of Figure 2f) of Fe-doped PANi.

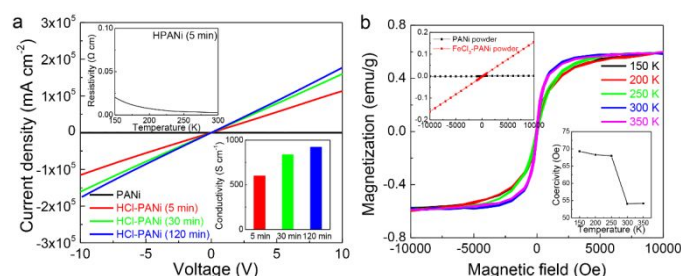


**Figure 3.** a) I-V curves of HPANi with different HCl doping periods at room temperature. Inset figures are the RT curve (left) and the calculated conductivities of each HPANi (right). b) MH loops of FePANi under different temperatures. Inset figures are the MH loops of PANi and FePANi powers at 300 K (left) and the coercivity of the FePANi (right).

Conducting HPANi and magnetic FePANi building layers play an important role in building molecular conducting magnet with the  $\pi$ -d interactions. The acid treatment increases electrical conductivity of PANi due to the proton-doping process.<sup>[13]</sup> As shown in Figure 3a, HPANi nanosheets show the increased conductivity comparing with the as-formed freestanding PANi nanosheet, which is transferred to the surface of 1M HCl aqueous solution for 5 min, 30 min, and 120 min. The 5-min HPANi offers a high conductivity of  $6.0 \times 10^2\text{ S cm}^{-1}$ , which can be further increased to  $8.4 \times 10^2\text{ S cm}^{-1}$  (30-min) and  $9.2 \times 10^2\text{ S cm}^{-1}$  (120-min), respectively (Figure S7). It should be noted that PANi in the emeraldine salt form shows an electrical conductivity with a range from  $10^{-3}$  to  $10^2\text{ S cm}^{-1}$  with varying conjugation length, doping level, and the type of dopant.<sup>[14]</sup> Notably, HPANi nanosheets prepared here through

supramolecular assembly show a remarkable high conductivity benefiting from the compact and ordering of the aniline chain. The resistivity-temperature (R-T) curve of HPANi layer in the inset of Figure 3a shows a low resistivity of  $0.02\ \Omega\text{ cm}$  at 150 K. Figure 3b shows the temperature dependent magnetization hysteresis (M-H) curves of FePANi layer, exhibiting ferromagnetic characteristics with a saturation magnetization of  $\sim 0.6\text{ emu/g}$ . It is known that the ferromagnetism requires not only magnetic moments (Figure S6) but also that the moments remain mutually aligned,<sup>[15]</sup> where the existence of spin alignment and d-d interaction between iron atoms is enhanced by the  $\pi$ -d interaction through the aniline chain. As shown in the left inset of Figure 3b, no magnetization is observed in PANi while a paramagnetic behavior is shown in the mixed Fe-PANi network. The coercivity shows an increased trend with the decrease of temperature as shown in the right inset of Figure 3b, indicating the enhanced ferromagnetism with the ferromagnetic coupling interactions in FePANi magnet under low temperature.

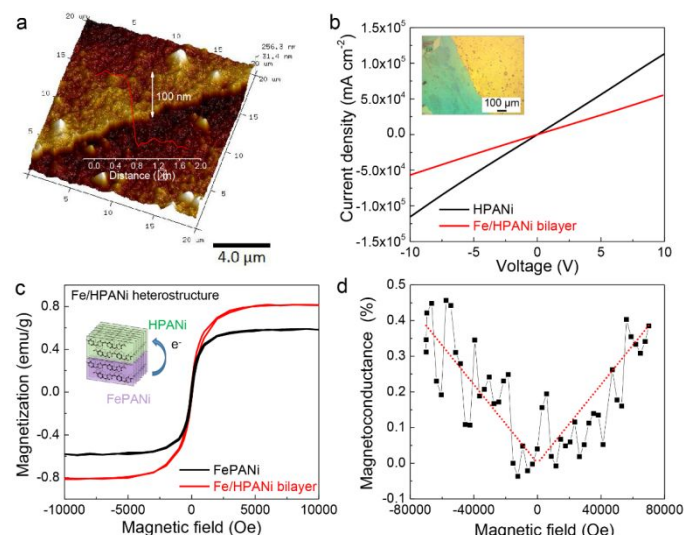


**Figure 4.** a) AFM image of the bilayer structure. Inset figure is the thickness measurement. b) I-V curve of FePANi/HPANi bilayer structure at room temperature. Inset figures are the corresponding optical microscopy image (left) and conductivities (right). c) MH loop of FeCl<sub>3</sub>/HCl bilayer structure and FePANi at 300 K. d) Magnetic conductance measurement of FePANi/HPANi bilayer at 180 K.

The coupling interactions between magnetic FePANi and conducting HPANi heterostructures (FePANi/HPANi) are resulted from the interfacial charge-transfer interactions. The interfacial structure is characterized by atomic force microscopy (AFM) shown in Figure 4a. The current-voltage curve of FePANi/HPANi bilayer indicates its comparable conductivity with the HPANi (Figure 4b). In comparison to HPANi with a conductivity of  $6.0 \times 10^2\text{ S cm}^{-1}$ , the FePANi/HPANi conducting magnet shows an average conductivity of  $3.5 \times 10^2\text{ S cm}^{-1}$ , while the FePANi/HPANi conducting magnetic heterostructure shows an enhanced saturation magnetization of  $0.80\text{ emu/g}$  which is 25% higher than that of FePANi (Figure 4c). The enhanced

magnetization of FePANI/HPANI could be resulted from the localized spin ordered states at the charge-transfer interface between metallic HPANI and FePANI layers,<sup>[16]</sup> where the induced charge from metallic layer of HPANI into magnetic layer of FePANI results in an increase of localized spin ordered states. The coupling between the magnetic and conducting FePANI/HPANI heterostructures is further evidenced by magnetoconductance behavior (Figure 4d). The change of conductance ( $\Delta G \%$ ) is calculated by:  $\Delta G \% = (G_H - G_0)/G_0 = (R_0 - R_H)/R_H$ , the  $G_H$  and  $R_H$  corresponds to the conductance and resistance under the magnetic field (H), respectively, and the  $G_0$  and  $R_0$  represent the conductance and resistance without the magnetic field. The conductance of FePANI/HPANI conducting magnet can be tuned under magnetic field with a symmetric enhancement by switching the direction of magnetic field. The conductance can be increased by 0.4% under the magnetic field of 70 kOe, at which the disrupted  $\pi$ -d interaction enhances electron mobility for the positive magneto-conductance of FePANI/HPANI.

## Conclusions

In conclusion, molecular conducting magnetic heterostructure is obtained in quasi-two-dimensional  $\pi$ -d aniline framework through supramolecular assembly in the presence of aniline and transition metal cations. The HPANI shows a metallic conductivity up to  $9.2 \times 10^2 \text{ S cm}^{-1}$ , while the FePANI shows ferromagnetism-like behavior with a saturation magnetization of  $\sim 0.6 \text{ emu/g}$  at 300 K. An enhanced magnetization of FePANI/HPANI heterostructure is achieved by coupling metallic and magnetic layers to induce localized spin ordered states at the charge-transfer interface and  $\pi$ -d interactions between metallic transport layer and magnetic layer, while a conductivity of  $3.5 \times 10^2 \text{ S cm}^{-1}$  is observed in such molecular conducting magnetic heterostructure. In addition, when a magnetic field is applied to molecular conductor, the aligned d electrons induce ferromagnetic ordering together with the disrupted  $\pi$ -d interaction for the enhanced electron mobility, leading to the magneto-conductance effect. Such materials-by-design and supramolecular assembly of hybrid materials with strong  $\pi$ -d interactions provide a general method for the development of organic conducting magnets.

## Conflicts of interest

There are no conflicts to declare.

## Acknowledgment

The U.S. Department of Energy, Office of Basic Energy Sciences, Division of Materials Sciences and Engineering supports S.R. under Award DE-SC0018631 (Organic conductors). Financial support was provided by the U.S. Army Research Office supports S. R. under Award W911NF-18-2-0202 (Materials-by-Design and Molecular Assembly).

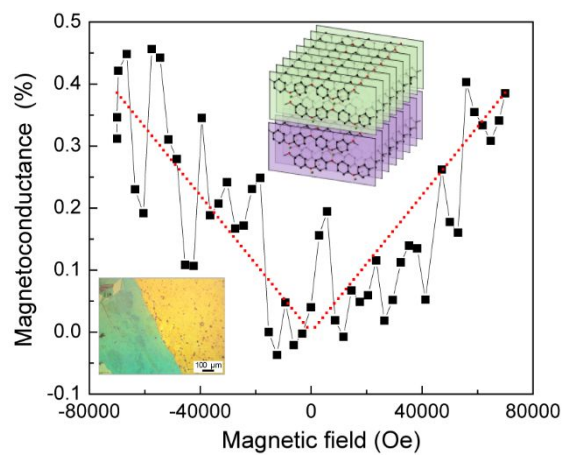
## Notes and references

- a) M. C. Beeler, R. A. Williams, K. Jimenez-Garcia, L. J. LeBlanc, A. R. Perry, I. B. Spielman, *Nature* **2013**, *498*, 201; b) W. Eerenstein, N. D. Mathur, J. F. Scott, *Nature* **2006**, *442*, 759; c) A. K. Powell, *Nat. Chem.* **2010**, *2*, 351; d) Y. N. Geng, H. Das, A. L. Wysocki, X. Y. Wang, S. W. Cheong, M. Mostovoy, C. J. Fennie, W. D. Wu, *Nat. Mater.* **2014**, *13*, 163; e) M. Warner, S. Din, I. S. Tupitsyn, G. W. Morley, A. M. Stoneham, J. A. Gardener, Z. L. Wu, A. J. Fisher, S. Heutz, C. W. M. Kay, G. Aeppli, *Nature* **2013**, *503*, 504.
- a) E. Coronado, P. Day, *Chem. Rev.* **2004**, *104*, 5419; b) T. Enoki, A. Miyazaki, *Chem. Rev.* **2004**, *104*, 5449.
- a) E. Coronado, J. R. Galán-mascaros, C. Gimenez-saiz, C. J. Gomez-garcia, S. Triki, P. Delhaes, *Mol. Cryst. Liq. Cryst.* **1995**, *274*, 89; b) E. Coronado, J. R. Galán-Mascarós, C. Giménez-Saiz, C. J. Gómez-García, S. Triki, *J. Am. Chem. Soc.* **1998**, *120*, 4671; c) J. R. Galán-Mascarós, C. Giménez-Saiz, S. Triki, C. J. Gómez-García, E. Coronado, L. Ouahab, *Angew. Chem. Int. Ed.* **1995**, *34*, 1460.
- a) S. A. Crooker, D. A. Tulchinsky, J. Levy, D. D. Awschalom, R. Garcia, N. Samarth, *Phys. Rev. Lett.* **1995**, *75*, 505; b) H. Akutsu, E. Arai, H. Kobayashi, H. Tanaka, A. Kobayashi, P. Cassoux, *J. Am. Chem. Soc.* **1997**, *119*, 12681.
- a) J. Huang, S. Virji, B. H. Weiller, R. B. Kaner, *J. Am. Chem. Soc.* **2003**, *125*, 314; b) X. S. Du, C. F. Zhou, Y. W. Mai, *J. Phys. Chem. C* **2008**, *112*, 19836; c) H. Zhang, X. Wang, J. Li, F. Wang, *Synth. Met.* **2009**, *159*, 1508.
- a) S. Mourdikoudis, L. M. Liz-Marzán, *Chem. Mater.* **2013**, *25*, 1465; b) C. J. Lockhart de la Rosa, R. Phillipson, J. Teyssandier, J. Adisojoso, Y. Balaji, C. Huyghebaert, I. Radu, M. Heyns, S. De Feyter, S. De Gendt, *Appl. Phys. Lett.* **2016**, *109*, 253112; c) C. Jiang, Z. Wang, H. Lin, Y. Wang, C. Luo, B. Li, R. Qi, R. Huang, X. Tang, H. Peng, *Colloids Surf., A* **2017**, *529*, 403; d) S. Soman, A. S. Chacko, V. S. Prasad, P. Anju, B. S. Surya, K. Vandana, *Carbohydr. Polym.* **2018**, *182*, 69.
- a) S. Li, C. Zhu, L. Tang, J. Kan, *Mater. Chem. Phys.* **2010**, *124*, 168; b) Y. Zhang, C. Zhu, J. Kan, *J. Appl. Polym. Sci.* **2008**, *109*, 3024.
- J. Yue, Z. H. Wang, K. R. Cromack, A. J. Epstein, A. G. Macdiarmid, *J. Am. Chem. Soc.* **1991**, *113*, 2665.
- B. C. Roy, M. D. Gupta, L. Bhoumik, J. K. Ray, *Synth. Met.* **2002**, *130*, 27.
- a) S. M. Roy, N. N. Rao, A. Herissan, C. Colbeau-Justin, *Polymer* **2017**, *112*, 351; b) W. S. Yin, E. Ruckenstein, *Synth. Met.* **2000**, *108*, 39.
- A. B. Rohom, P. U. Londhe, S. K. Mahapatra, S. K. Kulkarni, N. B. Chaurse, *High Perform. Polym.* **2014**, *26*, 641.
- Z. Moravkova, P. Bober, *Int. J. Polym. Sci.* **2018**, *1797216*, 1.
- a) A. Varela-Alvarez, J. A. Sordo, G. E. Scuseria, *J. Am. Chem. Soc.* **2005**, *127*, 11318; b) D. W. Hatchett, M. Josowicz, J. Janata, *J. Phys. Chem. B* **1999**, *103*, 10992; c) G. M. do Nascimento, M. L. A. Temperini, *J. Raman Spectrosc.* **2008**, *39*, 772.
- a) Y. Yang, S. Chen, L. Xu, *Macromol. Rapid Commun.* **2011**, *32*, 593; b) J. Jin, Q. Wang, M. A. Haque, *J. Phys. D: Appl. Phys.* **2010**, *43*, 205302; c) J. Stejskal, D. Hlavatá, P. Holler, M. Trchová, J. Prokeš, I. Sapurina, *Polym. Int.* **2004**, *53*, 294.
- I. M. L. Billas, A. Chatelain, W. A. Deheer, *Science* **1994**, *265*, 1682.
- F. A. Ma'Mari, T. Moorsom, G. Teobaldi, W. Deacon, T. Prokscha, H. Luetkens, S. Lee, G. E. Sterbinsky, D. A. Arena, D. A. MacLaren, M. Flokstra, M. Ali, M. C. Wheeler, G. Burnell, B. J. Hickey, O. Cespedes, *Nature* **2015**, *524*, 69.
- Q. Huang, S. Hu, J. Zhuang, X. Wang, *Chemistry* **2012**, *18*, 15283.

## Table of Content

### Molecular Conducting Magnetic Heterostructure

Feng Hu, Yong Hu, Yulong Huang, Changning Li, Ruizhe Yang, Shenqiang Ren\*



The doped quasi-two-dimensional aniline heterostructures through an interfacial assembly has been achieved with impressing conducting and magnetic properties.